Nonlinear Processes in Geophysics (1998) 5: 209–217

Nonlinear Processes in Geophysics

Advection of pollutants by internal solitary waves in oceanic and atmospheric stable stratifications

G. W. Haarlemmer[1] and W. B. Zimmerman[2]

[1]Department of Chemical Engineering, UMIST, P.O. Box 88, Manchester M60 1QD, England
[2]Department of Chemical and Process Engineering, University of Sheffield, Newcastle Street, Sheffield S1 3RD, England

Received: 26 August 1996 – Revised: 10 December 1997 – Accepted: 11 January 1999

Abstract. When a pollutant is released into the ocean or atmosphere under turbulent conditions, even a steady release is captured by large eddies resulting in localized patches of high concentration of the pollutant. If such a cloud of pollutant subsequently enters a stable stratification–either a pycnocline or thermocline–then internal waves are excited. Since large solitary internal waves have a recirculating core, pollutants may be trapped in the solitary wave, and advected large distances through the waveguide provided by the stratification. This paper addresses the mechanisms, through computer and physical simulation, by which a localized release of a dense pollutant results in solitary waves that trap the pollutant or disperse the pollutant faster than in the absence of the waves.

1 Introduction

In this paper, computer and physical simulations of atmospheric and oceanographic stratifications are disturbed by the introduction of dense tracers, simulating the nocturnal release of a dense gas from an industrial accident or the sudden release of a pollutant into an oceanographic pycnocline or thermocline. The simulation can also loosely model steady releases where the flow upstream of the stratification is turbulent. Intermittency breaks up the plume into localized clouds of pollutant that then enter the stratification separately. The simulations are of an initially static stratification, and thus the waveguide is unsheared. The purpose of this paper is to determine if there is a common asymptotic behaviour of solitary waves generated by the initial release in capturing the dense disturbance and advecting it along the waveguide large distances largely unchanged in concenetration. Alternatively, it can be determined if the solitary waves are an effective dispersal mechanism, resulting in low concentrations of pollutant smeared along the waveguide. This is an important question for regulatory bodies since legislation concerning industrial releases of dense toxic gases is written for daytime conditions, where convective rolls excited by solar heating lead to strongly turbulent, largely unstratified background conditions. In this case, turbulent wind tunnel studies have demonstrated generally rapid downwind mixing, with the inevitable intermittent behaviour leading to some outliers in high concentration (see e.g. Zimmerman and Chatwin, 1995). Nocturnal releases, however, are more likely to have low wind shear and strong stratification.

The solitary waves simulated in this paper emerge from initial disturbances designed to model industrial releases–dense gases from a tank rupture leading to a gravity current that breaks up into solitary waves or simply a localized, brief momentum source. In theses simulations, the strength and height of the stratification is varied. Waves are generated either by seeding a patch of fluid with vertical momentum or by introducing cold fluid into the waveguide. Mixing is monitored by "coloring" some of the fluid–numerically this is achieved by a passive tracer with low diffusivity. Initially, a mixed region occurs and one or more solitary waves emerges.

Although the initial conditions are well characterized, all theories for solitary wave evolution are asymptotic. They assume that the wave-like disturbance has a characteristic amplitude and wavelength, and thus a nonlinear evolution equation (NEE) is derived with solutions exhibiting, self-consistently, that amplitude and wavelength (see Zimmerman and Haarlemmer (1999a) for a discussion of the predictive capacity of existing NEEs to predict the properties of solitary waves). For practical purposes, one would like to correlate the size of the initial disturbance with the subsequent mixing downwind actuated by the emerging solitary waves. This paper discusses the extent to which such correlation is possible.

Correspondence to: Dr. Zimmerman

1.1 Solitary wave propagation

Although there are several NEEs for weakly nonlinear wave equations, in this paper motivation and interpretation are made with reference to shallow layer internal wave theory. Weakly nonlinear internal waves in shallow layers evolve according to the Korteweg-de Vries (KdV) equation. The phase speed can be predicted under the conditions of the simulations by solving a boundary value problem. The eigenvalue is the phase speed (c_0) of an infinitely long wave. This boundary value problem,

$$[\rho(c_0 - u(y))^2\phi_y]_y + \overline{\rho}N^2\phi = 0 \qquad (1)$$

with boundary conditions: $\phi(0) = \phi(y) = 0$, is known as the Taylor-Goldstein equation. Here y is the vertical coordinate of the eigenfunction ϕ; ρ is the density; $\overline{\rho}$ is the reference density, and N is the Brunt-Väisälä frequency. An increase in the strength of the temperature stratification will cause an increase in the phase speed of the wave. This is clearly shown in the simulations presented hereafter. When the wave is not infinitesimally small, the phase velocity c is corrected as follows:

$$c = c_0 + \frac{1}{3}\varepsilon\alpha h \qquad (2)$$

Here α is the coefficient of the nonlinear term in the evolution equation and h is the fluid height (more on this can be found in e.g. Rottman and Einaudi, 1993). The parameter ε is the relative size of the wave (η_{max}/h), the ratio of the maximum amplitude to the layer height.
In real fluids, viscous damping of the waves will play a (sometimes small) part in the evolution of the wave. Various damping mechanisms have been studied (see e.g. Zimmerman and Velarde, 1994 and 1996). In these simulations it is assumed that only bulk viscosity acts on the waves.

1.2 Organization of the paper

In section 2 an overview is given of fluid trapping observed in laboratory experiments and in the field. In addition, an indication about the size of solitary waves in natural waveguides is given. In the same section an overview of intensities of stratifications often found in natural waveguides is given. Section 3 outlines the numerical procedure and gives an overview of the simulations presented in section 4. In section 5 the experimental procedure and case studies are presented.

2 Literature overview

2.1 Large amplitude waves

A large amplitude solitary wave has closed streamlines. Weakly nonlinear waves have no such recirculation, but they do play a role in advection. Linear waves, however, give rise to no net displacement of fluid during propagation. The more nonlinear a wave, the larger the distances over which its convective processes are noticable.
Davis and Acrivos (1967) performed numerical simulations and laboratory experiments of solitary waves propagating on the interface of two miscible fluids. They found recirculation in waves with an amplitude larger than the stratified layer. Similar observations were made by Maxworthy (1980) and Amen and Maxworthy (1980). They created a mixed region with a tracer fluid that was released in a stratification. Initially the region spreads out as a gravity current. Subsequently, the gravity current breaks down into a train of solitary waves (see also Rottman and Simpson, 1989). Maxworthy observed that the leading wave transports the tracer away from the source. When the tracer is left behind this wave, a second trailing wave picks it up. This process becomes less pronounced with subsequent smaller trailing waves.
In atmospheric observations, large amplitude waves are common. Rottman and Einaudi (1993) reported that the amplitudes of the Morning Glory solitary waves in Northern Australia were up to half the height of the waveguide. Doviak and Christie (1989) report similar large amplitude disturbances. Many of the solitary waves observed in the lower atmosphere are highly nonlinear and are of the same order as the height of the waveguide. It turns out that small amplitude (weakly nonlinear) waves are very difficult to discern amongst the normal pressure variations in natural waveguides.

2.2 Modelling the waveguide

The model studied here is for a nocturnal inversion layer. During the night the temperature profile may become inverted due to radiative cooling of the earth surface. Due to normal adiabatic expansion, air cools as it rises. The potential temperature accounts for adiabatic cooling. A neutrally stratified atmosphere has a uniform potential temperature even though the absolute temperature may fall with height.
The strength and height of this inversion layer varies a great deal. Rees and Rottman (1994) report solitary waves propagating on the Brunt Ice shelf in Antarctica. They found a waveguide which was approximately 30m in height, with a temperature difference between top and bottom of about 20° C. These waves were found under the extremely stable conditions of the Antarctic winter. Elsewhere, the temperature profiles are usually less extreme. Ueda *et al.* (1981) examined the stability of the nocturnal atmosphere of the Tateno district in Japan. For the first 300m of altitude they find that the temperature increase varies typically from 1° C in the evening to 3°C in the early morning. These values are considerably smaller than those found for the Antarctic night. Mahapatra *et al.* (1990) report temperature increases of

No	Temp. profile	Height waveguide [km]	Amplitude disturbance[m] (at time [s])	ε [−]	Fr^* [−]	Description
1	10-11°C	2	408 (1000)	1.02	2.3	No background stratified up to 400m. passive tracer present
2	10-11°C	1	94.7 (800)	0.31	1.9	Background velocity 5m/s, stratified up to 300m, 5,000 Lagrangian particles, passive tracer component, grid moves at 5m/s.
3	10-14°C	1	129 (400)	0.43	1.1	Background velocity 5m/s, stratified up to 300m

Table 1. Numerical simulations performed, with the amplitude of the initial disturbance and the particularities of the simulations.

10-15°C in a waveguide of circa 3km, in Norman, Oklahoma. Other typical values found are 5°C per kilometre (Monserrat and Thorpe, 1992) on the Balearic Islands and 5-10°C in waveguides varying in height from 100-800m in Northern Australia (Smith *et al.*, 1986; Smith, 1988).
All of the stratifications reported above were associated with solitary waves. A trapping mechanism is needed to create a waveguide in which waves can propagate without radiating off vertically. Some trapping mechanisms are rapid changes of the temperature profile or shear layers.

3 Simulations

In the simulations, the full momentum equations are solved. The equations are solved using a general purpose equation solver PHOENICS©. The discretisation was done using a second order upwind scheme (QUICK, Leonard, 1988) to minimise numerical dissipation. More detailed accounts of the simulation methods and the equations solved are found in Haarlemmer and Zimmerman (1996) and in Appendix A. The viscosity of the gas is set to the natural viscosity of air (10^{-6} kg/ms). The density was computed using the ideal gas law

$$\rho = \frac{p}{T \cdot K} \tag{3}$$

where K=288.3m^2/(°C s^2). In this paper, potential temperature is used. The actual temperature (T_a), when adiabatic cooling is accounted for, is found from

$$T_a = T \left(\frac{p}{p_0} \right)^{(\gamma-1)/\gamma} \tag{4}$$

where γ is the gas compressibility and p_0 is the reference pressure.
Where a background velocity is applied, the pressure must be specified at the outflow boundary. It is assumed here that the pressure at the outflow boundary is built up solely from hydrostatic contributions. Further upwind in the flow, dynamic pressures are computed.
A characteristic dimensionless number in the flow is a modified Froude number $Fr^* = c/\sqrt{h\hat{g}}$. Here c is the characteristic velocity (phase speed), h is the height of the stratified layer and the reduced gravitational acceleration $\hat{g} = g(\rho_1 - \rho_2)/\rho_1$. Fr^* represents the dimensionless phase speed. This is concurs with the definitions found in Rottman and Simpson (1989) and Haase and Smith (1989).
Initially, the computational domain contains a stably stratified ideal gas at rest or in uniform motion. Then, a localized disturbance is introduced, evolving into a solitary wave. The domain is 10 to 40km in the horizontal direction and typically 1000m in the vertical. The computational mesh has 100 to 200 grid points horizontally, equally spaced apart. In the vertical direction there are 50 grid points. The initial stratification has a linear temperature profile in the lower part of the domain, the top part is left unstratified. The temperature profiles used in this study varied from 10-11°C (top layer 11°C uniform) to 10-14°C (top layer 14°C uniform). The height of the waveguide taken as either 1000m or 2000m.

4 Numerical results

Several simulations have been done with a variety of waveguides and waves. Some case studies will be highlighted (see Table 1). The first deals with a disturbance propagating through a stratification in a closed system. The second and third examples give a wave generated by introduction of cold air in a waveguide with a uniform background velocity. In both cases a tracer component was followed in time. The tracer is transported according to an advection-diffusion equation. The phase velocity of the simulated waves is compared to velocities predicted by the KdV theory. Koop and Butler (1980) argued that a wave propagating on a stratified layer with a depth of $1/6^{th}$ of the total depth of the fluid can still be described with the shallow fluid approximation.

4.1 Simulation 1: Closed system

In this first simulation, a weakly stratified waveguide is perturbed with a vertical velocity component. The wave is initially of the same order of magnitude as the stratified part of the waveguide ($\varepsilon = 1.02$). The mesh has 200 grid points horizontally (40 km) and 50 vertically (2km). In the first time step a patch of 5 × 5 cells (1000 × 100m) was perturbed with a vertical velocity of 50m/s directed downwards. In the same patch a tracer was introduced in the fluid. The disturbance was left to

Fig. 1. The temperature profile (left), the tracer concentration (center) and vertical velocities (right) after 1000s in simulation 1.

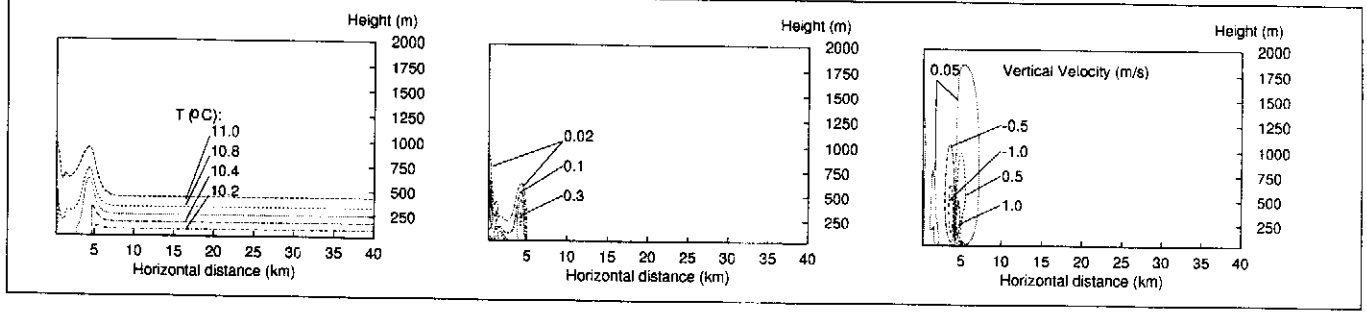

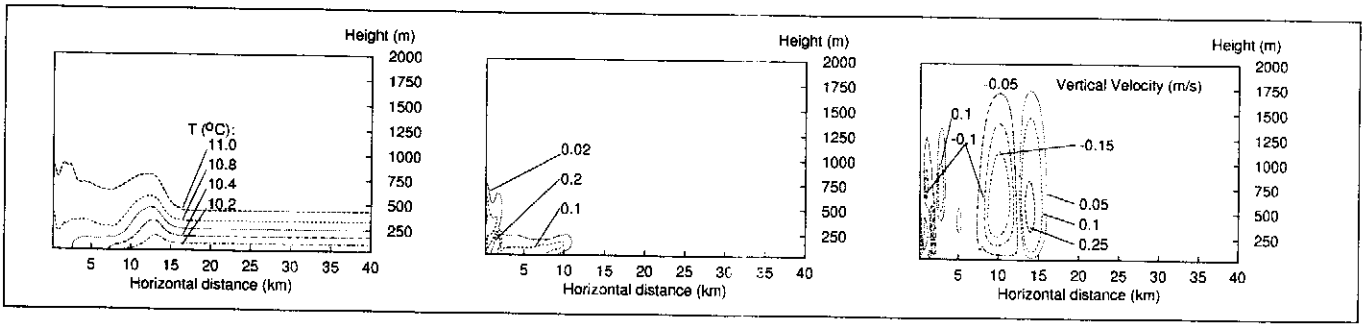

Fig. 2. The temperature profile (left), the tracer concentration (center) and vertical velocities (right) after 4000s in simulation 1.

develop into a train of solitary waves.

A mixed zone with strong vertical velocity components is created. Although initially no horizontal momentum is introduced, shortly thereafter a strong horizontal wind arises. This mixed zone flows into the stratification as a gravity current, (see Fig. 1). It is clear that the head of the gravity current develops into a large amplitude wave. The tracer is trapped in the wave and is convected away from the site of the disturbance. The contour lines of the tracer clearly show the wave-like structure of the disturbance.

When the simulation is taken further in time, the weak viscous and dispersive forces have acted on the leading solitary wave in the gravity current. Recirculation is still visible after 2000s. The wave amplitude decreases until recirculation disappears completely. The resulting wave is weakly nonlinear and will propagate away without having a significant effect on the tracer, as shown in Fig. 2.

The phase speed of the wave is computed to be 2.7m/s. This is somewhat higher than the phase speed of 2.3m/s predicted by the weakly nonlinear KdV theory for this waveguide and amplitude.

This simulation clearly shows that the disturbance initially creates a highly nonlinear wave with the ability to *trap and transport a part of the fluid.* As the wave evolves, it decreases in amplitude. In smaller waves, less fluid is trapped, and slowly the tracer is expelled from the wave. *When the wave becomes sufficiently small it can be described by the weakly nonlinear KdV theory.* The phase speed predicted by this theory is smaller than the observed phase speed.

4.2 Simulation 2: Uniform background wind

In this simulation, the wave was created in a waveguide with a background velocity of 5m/s. The potential temperature varied from 10-11°C in the lower layers up to 300m altitude and was left unstratified above. A wave was created by introducing air with a temperature of 10°C at a velocity of 17m/s for 40s. This created a disturbance that propagates downwind. The frame of reference travels at the same velocity as the background wind. During the simulation the coordinates of 5,000 Lagrangian fluid elements were traced in time. The particles travel along the streamlines which remain constant during a time step. Between timesteps of the simulation algorithm new locations of the particles are computed in two steps. These particles were located near the origin of the wave (see the cloud at t=0 in Fig. 3).

It is clear that the wave in this simulation is not as large as the wave in Simulation 1. There is no recirculation visible in the isotherms. Furthermore, the vertical velocities of the waves are small – the same order of magnitude as the velocities in Fig. 3. There is a large depression trailing the wave and this appears to push the tracer forward. This is also shown by the motion of the Lagrangian fluid elements. The cloud of particles is pushed away from the source. Some rotational element is present in the center of the wave though it is rather weak.

The phase velocity in this simulation is initially very high (5m/s) but then rapidly decreases to 1.85m/s. The weakly nonlinear theory predicts 1.95m/s. As can be seen in the figure for the concentration the center of

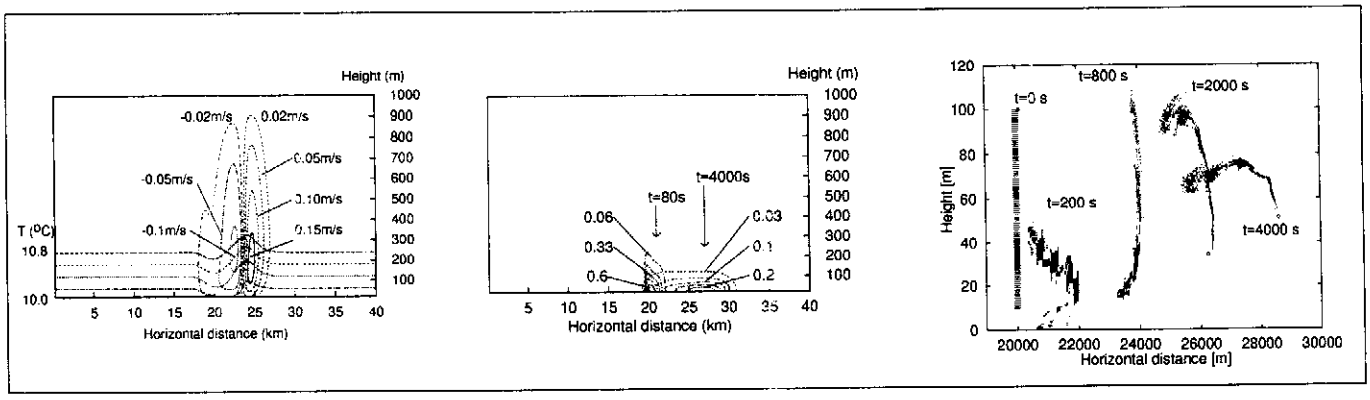

Fig. 3. The temperature profile with vertical velocities after 800s (left), the tracer concentration (center) and the location of 5,000 Lagrangian fluid elements (right) in simulation 2.

the tracer, with the highest concentration, travels at a velocity of 1.75m/s. The Lagrangian fluid elements display a similar behaviour.

The generation of this wave was fundamentally different from the first simulation. An amount of cold air was introduced in the waveguide creating a wave. The wave propagates away from the source with a velocity close to the phase speed predicted by the weakly nonlinear theory. *The wave clearly convects the perturbing fluids away from the source.* As the wave decreases in amplitude, convective effects become weaker and a long trail of the tracer is the result. A large release of dense gas, as after an industrial accident in a nocturnal inversion layer, may trigger a wave of this kind. *The pollutants thus introduced may travel significantly faster (or slower, if the wave opposes the wind) than can be expected on the basis of background wind velocities.*

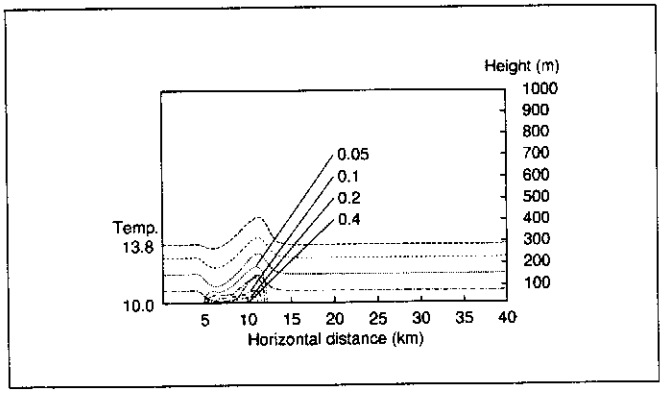

Fig. 4. Temperature profile and concentration profile in simulation 3 after 400s

4.3 Simulation 3: Strong stratification

In a stronger stratification, nonlinearity will play an increasingly important role. In addition the phase speed of the waves should increase as predicted by nonlinear theory. In this simulation a shearless stratification was set up. The lower 300m has a linear temperature profile increasing from 10°C to 14°C. The top 700m was left unstratified. To maintain numerical stability at the boundaries, the grid was held stationary. A disturbance was released with a velocity of 20m/s for 40s (temperature 10°C, concentration tracer unity). This creates a wave with an amplitude of 129m.

The disturbance develops into a train of solitary waves as the weakly nonlinear theory predicts. The head of the tracer appears to be pushed forward by the wave although as the wave decreases some of the tracer slips out of the back of the wave. The presence of the solitary wave appears to have a significant effect on the horizontal spreading of the tracer. The leading wave develops a phase speed of 9.5m/s. The KdV theory predicts in this case a phase speed of 9.2m/s. The tracer velocity is 8.3m/s, slightly slower than the wave but still consid-

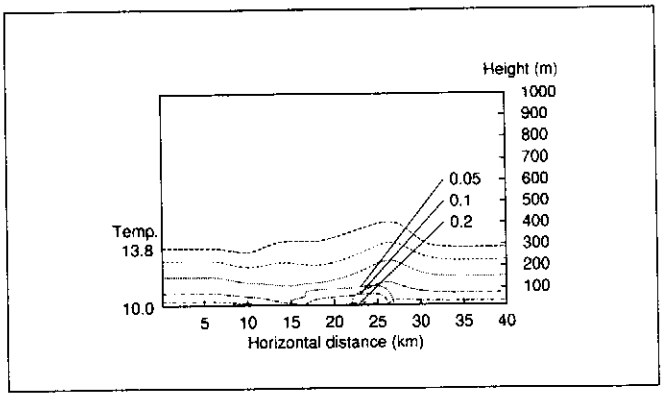

Fig. 5. Temperature profile and concentration profile in simulation 3 after 2000s

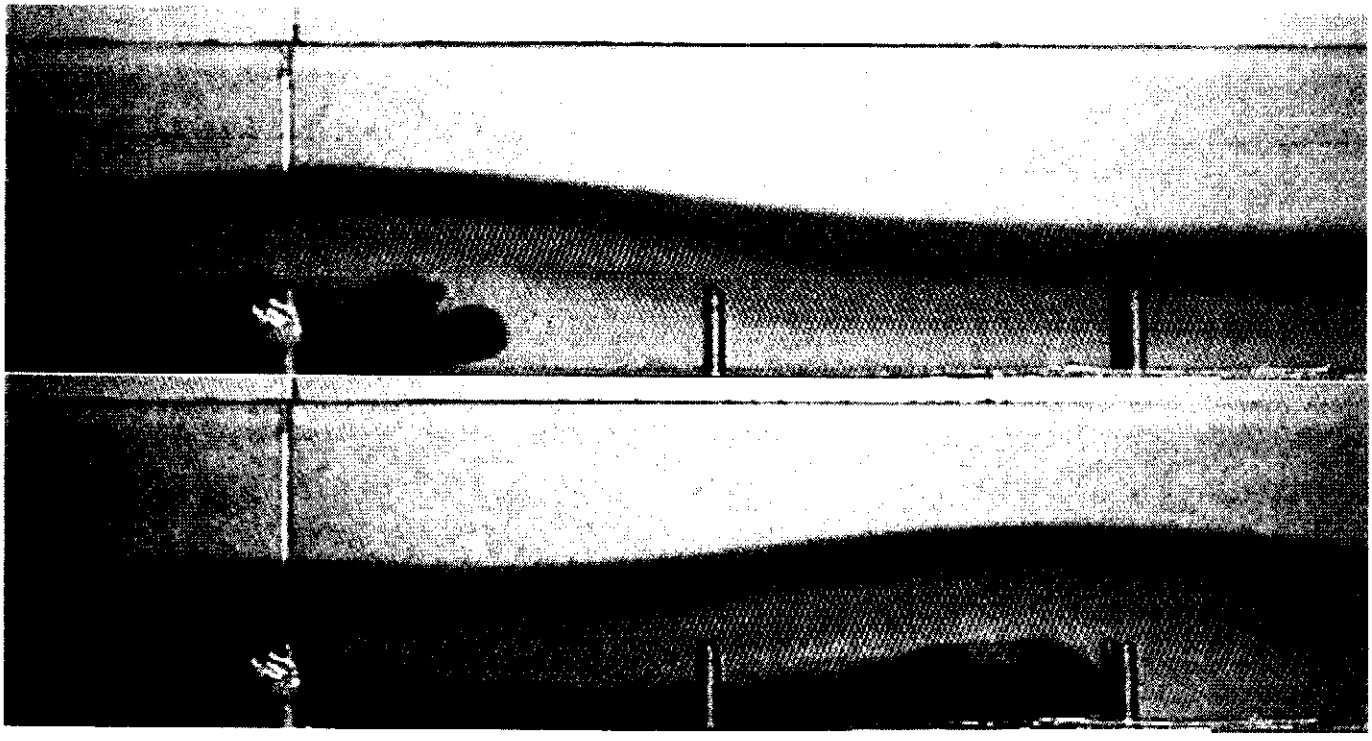

Fig. 6. Video stills of experiment 1. Top frame: Wave at t=t $_1$. Bottom frame:Wave at t=t_1+5s. A 40cm section of the wave tank, 40cm from the origin of the wave. The concentration pattern is similar to the simulation in Fig. 5.

erably faster than the background wind (5m/s).
More solitons are generated in stronger stratifications. The leading soliton traps the perturbing cold fluid in the same way as in simulation 2. The phase speed is in good agreement with the weakly nonlinear theory. *Stronger stratifications imply that pollutants are convected faster* when trapped in a wave of this kind.

5 Experiments: Solitary waves with recirculation

The experimental system, a wave tank with denisity probes and a dedicated optical system, was purpose-built. The tank is a rectangular channel made of transparent U-PVC. The dimensions are 200×25×10cm. Data is collected using conductivity probes and a video camera. The results are presented in the form of video stills. A stratification is set up by introducing fluids of different densities in the tank. First fresh water is put in place after which batches of brine with increasing densities and different colours are introduced near the bottom of the tank. The different fluids organise themselves vertically with the lightest fluid on the top. The interfaces are miscible and so a nearly linear stratification can be set up with a known density distribution. The intensity field from light transmission through the tracer dyes forms a gray scale correlated with density.
It is possible to generate solitary waves in a great many ways. Almost any disturbance in stably stratified fluids produces waves of some sort. Gravity currents are created by an area of fluid with a high density separated from the stratification. When the separation is removed, the dense fluid flows into the stratification creating a train of solitary waves (see also Maxworthy, 1980 and Rottman and Simpson, 1989). In most experiments a localised solitary wave is created by introducing a small but finite volume of dense fluid in the stratification. This results in a solitary wave without generating a gravity current.

5.1 Shallow layers

A typical example of a wave propagating in a relatively shallow layer is given first. The highest fluid layer is undyed. The second and third fluid from the top were dyed. The interface between the different layers blurred somewhat. The stratification was therefore nearly linear. The tank was filled with fluids (from top to bottom)with heights (cm) and densities (kg/m^3): 4, 998; 1, 1008; 1, 1015 and 1, 1023.
A wave was created by introducing a finite amount (100ml) of dyed dense fluid (1050 kg/m^3). This disturbance evolved into a train of solitary waves. The fluids that caused the disturbance were trapped and convected away from the source. It is the presence of the waves that cause this horizontal spreading of the fluids. In the absence of the waves the dense fluids developed a very weak gravity current that did not produce any significant wave motion. The video stills of this experiment are given in Fig. 6. The black fluid in the experiment is

in fact not a gravity current, but a trail of dye left by the leading wave. The leading wave has a strong recirculation that causes mixing of the dense fluid with the higher layers. The dye and thus the dense fluid penetrates into the stratification. This gives the dye pattern the appearance of a gravity current.
From the wave in Fig. 6 it is clear that the fluids in the center are recirculating. This recirculation causes local shear instabilities that form the irregular structures in the center of the leading wave. It appears that this is the only mixing mechanism that is available. The amplitude of the wave measured at the top of the stratification is $A = 1.3\text{cm}$, with $\varepsilon = A/H = 0.19$. The surface of the fluids in the wave tank remained calm even though large amplitude waves were propagating under the surface.
The phase velocity of the wave in Fig. 6 is circa 6cm/s. The KdV theory predicts a long wave phase velocity of $c_0 = 4.7\text{cm/s}$. The coefficient of the nonlinear term is $\alpha = \varepsilon 1.4\text{s}^{-1}$. These are used in the expression for the actual phase velocity: $c = c_0 + \frac{1}{3}\alpha H$, with $H = 7\text{cm}$ total fluid depth. The prediction for phase velocity is $c = 5.2\text{cm/s}$. Phase velocity is under-predicted by the weakly nonlinear theory. The wave has a recirculation and is therefore strongly nonlinear. In addition the stratification was assumed to be linear in the theory. This assumption may only be an idealization of the stratification in the experiments.

5.1.1 Wave evolution in deep water

The second deep fluid wave experiment deals with a light un-dyed stratification. The stratification was set up with two fluids. The top fluid was 5cm of fresh water (998 kg/m^3) with the bottom layer more dense at 1008 kg/m^3. The wave was created using a dense fluid (1050 kg/m^3), dyed with black negrosine. The result of the experiment was a wave propagating through the stratification and advecting some of the original tracer fluid.
The structure of the wave is more complex than a simple sech^2; after the initial wave there is a slight depression. In addition it is clear that tracer fluid escapes from the leading wave. This gives the appearance of a gravity current, when in fact the leading solitary wave is not forced by a gravity current. The wave develops a bore like appearance because some dyed fluids mix with the upper layer and slip out of the leading wave. Streaks of dye near the leading wave indicate shear instabilities.
The phase velocity of the wave in Fig. 7 is 3cm/s. When it is assumed that the density profile is nearly linear the shallow fluid theory predicts a long wave phase velocity of 2.6cm/s with the coefficient of the nonlinear term $\alpha = \varepsilon 2.5\text{s}^{-1}$. Assuming the wave amplitude $A \approx 1\text{cm}$, the phase velocity is given by $c = c_0 + \frac{1}{3}\alpha H = 3.3\text{m/s}$. This is somewhat over predicted. The estimate for the amplitude of the wave and the degree of nonlinearity can account for the difference.

5.2 Summary

These two experiments, and many others like them (see Haarlemmer (1997)), show that the mechanisms identified in this paper do indeed occur in real fluids. The recirculation slowly disappears. *The wave is very effective in horizontal dispersion of the perturbing fluids.* The fluid surface is not significantly affected by the passage of the internal wave and remains calm.

6 Discussion and Conclusions

Clearly, this paper gives only a cursory presentation of the experimental investigation, reporting qualitative features in a handful of case studies about mixing and dispersion by internal solitary waves. It is regrettable that more quantitative measures of mixing and dispersion are not presented. There are two chief reasons.

1. The initial releases were not easy enough to control for reproducibility. Indeed, the asymptotically emerging solitary waveforms were typically rather different for the initial conditions of nominally the same parametric description in the experiments.

2. Neither the density probes nor the optical system were sufficiently accurate to give reliable measures of density disturbance.

The limited scope of the experiments was to provide some physical validation of the computer simulations, which has been achieved. The much more quantitative simulations have been surprisingly unable to draw generalizations about dispersion *from the initial releases* other than small amplitude solitary waves are efficient at short range mixing, and large amplitude solitary waves disperse fluids much further and fairly uniformly due to the slippage from the aft of the solitary wave. Eventually, the tracer fluid is completely released after a fixed length.
The difficulty in making generalizations is twofold:

1. The characterization of the initial disturbance. The simulations give an idealization, where the experiments have internal heterogeneity.

2. The lack of a predictive theory for *internal* solitary waves emergent from an initial disturbance.

There is an inverse scattering paradigm for solitary waves satisfying the Korteweg-de Vries equation–a train of solitons emerges from an initial disturbance with the largest and fastest leading, and the train follows in descending order of amplitude. Indeed, atmospheric observations have mimicked this paradigm [Doviak and Christie, 1989]. However, each emergent solitary wave from an initial disturbance sets up its own Korteweg-de Vries equation due to the parametric dependence of the coefficients of the KdV equation on its amplitude and wavelength. Thus, there is no unique KdV equation that

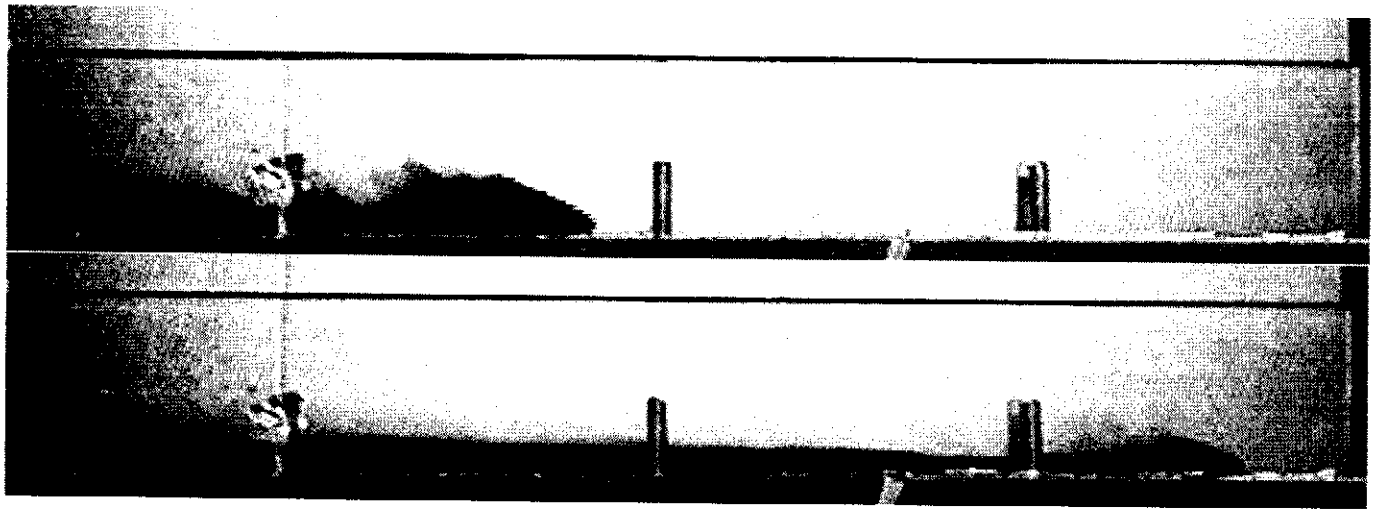

Fig. 7. Video stills of experiment 3. Top frame: Wave at t=t $_1$. Bottom frame:Wave at t=t_1+7s. A 40cm section of the wave tank, 40cm from the origin of the wave.

governs the horizontal propagation in the waveguide of all of the emergent internal waves. Given our experience with setting up solitary waves in wavetanks, it is clear that the emergent solitary waves are sensitive to fluctuations in the initial condition. The extent to which the inverse scattering transform provides meaningful information about the dynamics of the emergent internal solitary waves is the subject of our companion paper [Zimmerman and Haarlemmer, 1999b].

It was shown in the simulations and the experiment that solitary waves do indeed play a role in the convection of fluids. The effects are stronger for simulations where the wave was created by introducing dense fluids in a waveguide. After creation of the wave some of the perturbing tracer fluids are picked up and transported away from the source. This mechanism was confirmed by the experiments.

Waves larger than weakly nonlinear display no uniform waveform on every streamline. This implies that there is no unambiguous criterion for the size (such as $\varepsilon > 1$) of the wave for which convection by waves is important. Furthermore, this defies the explanation of all dynamical theories based on separation of variables.

In the experiments, the fluid surface is not significantly disturbed by the presence of internal waves. Thus "rigid lid" boundary conditions in the simulations are therefore not too severe a restriction on the dynamics of the waves. The proposed mechanisms may be of particular interest in the nocturnal inversion layer. After an industrial accident at night a large wave may be triggered and transport fluids away from the source much faster than can be expected on the basis of the background velocity.

Acknowledgements: The authors wish to thank C.I. Christov and M.G. Velarde for helpful discussions. Financial support from a UMIST postgraduate fellowship is gratefully acknowledged. The second author is grateful to NATO for collaborative research grant 940242.

Equation:	ϕ	Γ	S
Momentum	$\mathbf{u} = (u, v, w)$	η	$-\nabla(p)$ +gravity
Continuity	1	0	Boundary Conditions
Energy	T	k	Source
Concentration	C	$\mathcal{D}$	Source

Table 2. Variables used for the generalisation of the governing equations

Appendix A: Discretisation Scheme

A commercial computational fluid dynamics package, PHOENICS©, was used. The transient simulations are performed in a two dimensional domain. The discretisation scheme for governing equations is given below for a one dimensional situation. The value of the variable in cell p can be given as a function of the values of the neighbouring cells. The previous time step is treated as a neighbouring cell. Effectively, time is treated as an extra spatial dimension. The equations all have the same form and a general variable ϕ can be defined. The generalised governing equations are be given by:

$$\frac{d(\rho\varphi)}{dt} + \nabla \cdot (\rho \mathbf{u}\phi) - \nabla \cdot [\Gamma \nabla(\phi)] = S \tag{5}$$

All equations have the same form and are discretised in a similar fashion with a second order upwind finite difference scheme: QUICK (Leonard, 1988). The variables and source terms S are given in Table 2.

Now (5) can be integrated once in the control volume. For a 1D steady state example this yields:

$$[(\rho u\phi)_e - (\rho u\phi)_w] - \left[\left(\Gamma_\phi \frac{d\phi}{dx}\right)_e - \left(\Gamma_\phi \frac{d\phi}{dx}\right)_w\right] = \int_e^w S_\phi dx \tag{6}$$

The index e means the value at the cell face 'east' (right) of node P, w indicates the cell face 'west' (left) of P.

The value of ϕ_f (where f is either e or w) must now be computed from a finite difference approximation such as QUICK:

$$\phi_e = \frac{1}{2}(\phi_P + \phi_D) - \frac{1}{8}(\phi_D - 2\phi_P + \phi_U)$$

Here D stands for downwind and U for upwind nodal points. When this approximation is used in (6) it is possible to express the value of ϕ_P in terms of values of its neighbouring cells. The time integration is fully implicit. The matrix equations that now arise are solved using a conjugate gradient solver. The algorithm used to solve the pressure linked equations is SIMPLEST (see e.g. Patankar, 1980).

The numerical setup has been tested for accuracy by doubling the number of grid points and time steps for a given simulation. It was found that the scheme presented here was stable and sufficiently accurate for the given number of grid points. Typical simulations take 24-50 hours on HP-700 workstations.

References

Amen, R. and Maxworthy, T., "The gravitational collapse of a mixed region into a linearly stratified fluid". *J. Fluid Mech.*, **96**:65–80, 1980.

Benney, D.J., "Long non-linear waves in fluid flows". *J. Math. Phys.*, **45**:52–63, 1966.

Christie, D.R., "Long nonlinear waves in the lower atmosphere". *J. Atmos. Sci.*, **46** (11):1462–1491, 1989.

Davis, R.E. and Acrivos, A, "Solitary waves in deep water". *J. Fluid Mech.*, **29** :593–607, 1967.

Doviak, R.J. and Christie D.R., "Thunderstorm generated solitary waves: A wind shear hazard". *J. Aircraft*, **26** (5):423–431, 1989.

Haarlemmer, G.W., "Dynamics of internal waves in ocean and atmosphere." Ph.D. thesis, University of Manchester Institute of Science and Technology, 1997.

Haarlemmer, G.W. and Zimmerman, W.B., "Enhancement of mixing by internal solitary waves in stratified flows". Proc. Fluid Mixing 5, ICheme Symposium Series No 140, pp 225–235, 1996.

Haase, S.P. and Smith, R.K. "The numerical simulations of atmospheric gravity currents part II, environments with stable layers". *Geophys. Astrophys. Fluid Dyn.*, **46**:35-51, 1989.

Leonard, B.P., "Simple high-accuracy resolution program for convective modelling of discontinuities". *Int. J. Num. Meth. Fluids* , **8**:1291-1318, 1988.

Mahapatra, P.R., Doviak, R.J. and Zrnić, D.S., "Multisensor observations of an atmospheric undular bore". *Bull. Am. Met. Soc.*, **72**(10):1468–1480, 1990.

Maxworthy, T, "On the formation of nonlinear internal waves from the gravitational collapse of mixed regions in two and three dimensions". *J. Fluid Mech.*, **96**:47–64, 1980.

Monserrat, S. and Thorpe, J., "Gravity wave observations using an array of microbarographs in the Balearic Islands". *Q. J. R. Met. Soc.*, **118**:28 pp, 1992.

Patankar, S.V., Numerical heat transfer and fluid flow. Hemisphere Publishing corporation, New York, 1980.

Rees, J.M. and Rottman, J.W., "Analysis of solitary disturbances over an Antarcic ice shelf". *Bound.-Lay. Met.*, **69**:285–310, 1994.

Rottman, J.W., and Einaudi, F., "Solitary waves in the atmosphere". *J. Atmos.Sci.*, **50** (14):2116–2136, 1993.

Rottman, J.W. and Simpson, J.E., "The formation of internal bores in the atmosphere: A laboratory model". *J. Roy. Met. Soc.*, **115**:941–963, 1989.

Smith, R.K., "Travelling waves and bores in the lower atmosphere. The 'Morning Glory' and other related phenemona". *Earth Sci.*, **25**:267–290, 1988.

Smith. R.K., Coughlan, M.J. and Lopez, J.L., "Southerly nocturnal wind surges and bores in north easter Australia". *Month. Wea. Rev.*, August 1986.

Ueda, H., Mitsomoto, S. and Komori, S., "Buoyancy effects on the turbulent transport processes in the lower atmosphere". *Quart. J. R. Met. Soc.*, 107:561–578, 1981.

Zimmerman, W.B. and Chatwin, P.C. , "Fluctuations in dense gas concentrations measured in a wind-tunnel." *Boundary Layer Met.*, **75** :321-352, 1995.

Zimmerman, W.B. and Haarlemmer, G.W., "Tracer dispersion by internal solitary waves in stable stratifications." Mixing and Dispersion in Stably Stratified Flows, Proceedings of the IMA, New Series Number 68, 373–392, P.A. Davies, ed., 1999a.

Zimmerman, W.B. and Haarlemmer, G.W., "Internal gravity waves: Analysis using the periodic, inverse scattering transform". *Nonl. Proc. Geophys.*, in press, 1999b.

Zimmerman, W.B. and Velarde, M.G., "Nonlinear waves in stably stratified dissipative media- solitary waves and turbulent bursts". *Phys. Scr.*, **T55**:111-114, 1994.

Zimmerman, W.B. and Velarde, M.G., "On the possibility of wave-induced chaos in a sheared, stably stratified fluid layer". *Nonl. Proc. Geophys.*, **1**:219–223, 1994.

Zimmerman, W.B. and Velarde, M.G., "A centre manifold approach to solitary internal waves in a sheared, stably stratified fluid layer". *Nonl. Proc. Geophys.*, **3**:110–114, 1996.